

An Analysis of Chlorophyll Fluorescence Algorithms for the Moderate Resolution
Imaging Spectrometer (MODIS)

Ricardo M. Letelier and Mark R. Abbott

College of Oceanic and Atmospheric Sciences
Oregon State University
Ocean. Admin. Build. #104
Corvallis, OR 97331-5503

Abstract

Next-generation ocean color sensors will include channels to measure passive chlorophyll fluorescence as well as traditional channels that use radiance ratios to estimate chlorophyll concentration. Because the chlorophyll fluorescence signal is small, these sensors have significantly higher signal to noise ratios in the channels used to measure fluorescence. Small changes in sensor performance, atmospheric transmissivity, and fluorescence efficiency could potentially result in significant changes in the performance of the fluorescence algorithms. We perform a sensitivity analysis on the present MODIS algorithms and derive the minimum chlorophyll concentrations that can be observed for various combinations of sensor performance, atmospheric conditions, and phytoplankton physiology. We show that the present sensor specifications will allow us to observe fluorescence at chlorophyll concentrations as low as 0.5 mg/m^3 at the full resolution of the sensor (nominally 1 km^2 at nadir) under optimum viewing conditions. Although sensor changes have only a small impact on the individual bands used to calculate fluorescence, the total performance of the fluorescence algorithm can vary considerably. We recommend some changes in the present MODIS specifications that will improve the performance of the MODIS fluorescence algorithms.

Introduction

Fluorescence by the main light-harvesting pigments of phytoplankton is one of the main pathways for the deactivation of photosystem II (PS II) which is responsible for over 95% of chlorophyll fluorescence. This portion of the photosynthetic cycle is responsible for the splitting of water molecules and the formation of oxygen. Nicotinamide adenine dinucleotide phosphate (NADP) reduction takes place in photosystem I (PS I), and this photosystem is only weakly fluorescent. Together, PS I and PS II are known as the “light” reactions as they require light energy to proceed. The amount of fluorescence is a complicated function of light capture by chlorophyll and the rate of electron flow between PS II and PS I. Thus much attention has been focused on the use of fluorescence to estimate chlorophyll concentrations and primary productivity. An excellent summary of fluorescence can be found in Kiefer and Reynolds (1992).

The coupling between fluorescence and the rate of photosynthesis has intrigued researchers for many years. Samuelsson and Öquist (1977) suggested that the addition of the photosynthetic inhibitor [3-(3,4,4-dichlorophenyl)-1,1-dimethyl urea] (DCMU, a common herbicide) could be used to separate the effects of light absorption (as an indicator of chlorophyll concentration) from light utilization (photosynthesis). Although DCMU does block electron flow and thus stimulates fluorescence, there are numerous other processes that affect fluorescence yield.

Again, DCMU-induced fluorescence, as with the basic fluorescence method, can be used as an indicator of various physiological processes within the cell, but the relationship is complex (Prézelin 1981).

Recent research has focused on the use of sun-stimulated fluorescence to estimate primary productivity (e.g., Chamberlin et al., 1990; Kiefer et al., 1989; Kiefer and Reynolds, 1992; Stegmann et al., 1992; Chamberlin and Marra, 1992; Abbott et al., 1995). Although there is a link between the rate of productivity and the rate of fluorescence, it is not straightforward. As noted by Falkowski and Kolber (1993), the quantum efficiency of photosynthesis varies inversely to the quantum efficiency of fluorescence. However, there is no simple predictor of photosynthetic quantum efficiency. Falkowski and Kolber (1993) suggest that sun-stimulated fluorescence may not work over the wide range of oceanic conditions.

Early measurements of upwelled radiance in natural waters showed the presence of a distinct peak in the spectrum centered at 683 nm. The observed deviation around 683 nm from the expected sea surface leaving radiance spectrum of pure water has been attributed to the characteristic peak of chlorophyll fluorescence (Neville and Gower, 1977; Gordon, 1979). Smith and Baker (1978; 1981) clearly show this phenomenon using high quality, narrow bandwidth radiance measurements. This effect has been studied using in situ

observations by numerous researchers, including Gordon (1979), Topliss (1985), Topliss and Platt (1986), Fischer et al, (1986), and Kishino et al. (1984).

Neville and Gower (1977) described the first measurements of sun-stimulated fluorescence from aircraft and suggested using this signal to estimate chlorophyll concentrations from aircraft and satellites. The principle was identical to the basic fluorometer used in aquatic studies; a light source (in this case, the Sun) would stimulate the fluorescence reactions which would then be measured by a narrow band detector. Known as solar or sun-stimulated fluorescence and occasionally as passive or "natural" fluorescence, this technique complements the more traditional method of ocean color remote sensing which is based on radiance ratios in the blue/green portion of the spectrum (Clark, 1981). Sophisticated aircraft sensors have been developed with more bands and narrower bandwidths, culminating with the FLI (Fluorescence Line Imager) instrument that was optimized for fluorescence measurements (Gower 1980; Gower and Borstad 1981; Gower and Borstad 1990). Similar sun-stimulated fluorescence measurements have been made in Germany (Fischer and Kronfeld, 1990; Fischer and Schlüssel, 1990).

These aircraft and ship studies prompted plans to develop satellite sensors that would be capable of measuring chlorophyll fluorescence from low Earth orbit. The first such sensor will be MODIS (Moderate Resolution Imaging Spectrometer) which will be launched in 1998 as part of the National Aeronautics

and Space Administration's (NASA) Earth Observing System (EOS). This will be followed in by the Medium Resolution Imaging Spectrometer (MERIS) which will be launched by the European Space Agency (ESA) and the Japanese Global Land Imager (GLI) in 2000. This paper will explore the effects of changes in sensor performance, atmospheric transmissivity, and phytoplankton physiology on the performance of fluorescence algorithms. We will focus on MODIS as its performance characteristics are more fully defined at this time. However, these results will be generally applicable to MERIS and GLI as well.

Fluorescence Algorithms

The general algorithm form developed to estimate the fluorescence signal, also called fluorescence line height (FLH), relies on three wavelength readings (Fig. 1). One of these wavelengths is centered on the chlorophyll fluorescence maximum (approximately 683 nm). The remaining two wavelengths, required for backscatter correction, are used to form a baseline below the fluorescence peak with one band at a shorter wavelength than the peak and one band above. The FLH approach has been developed by Gower (1980). FLH is less sensitive to interference caused by the presence of other absorbing suspended matter commonly found in surface waters, and does not saturate at high chlorophyll concentrations as do algorithms that rely radiance measurements at 443 nm. Early results using airborne passive detectors suggest that there is a strong agreement between the magnitude of the FLH and the chlorophyll concentration

in surface waters (Gower and Borstad, 1981; Amann and Doerffer; 1983; Hoge et al., 1987). However, because the fluorescence intensity signal can vary independently from chlorophyll concentration, care must be taken when interpreting spatial and temporal changes in FLH. As suggested by Borstad et al. (1985), combining the FLH measurement with an independent estimate of chlorophyll concentration (using the radiance ratio approach) may provide a powerful tool to assess the physiological state of the phytoplankton.

Although the FLH algorithm is straightforward, there are three processes that we must consider before we can interpret FLH estimates from MODIS. The first process involves scattering and absorption in the atmosphere. Radiance leaving the ocean undergoes several modifications before it reaches the sensor. There is the addition of reflected sun and sky light from the sea surface and scattered light from the intervening atmosphere. There is also absorption by gases in the atmosphere. Scattering effects are most pronounced at shorter wavelengths, but the fluorescence line is located in region of the spectrum where there are several narrow absorption features. In particular, there is an oxygen absorption band at 687 and 760 nm as well as a water vapor absorption band at 730 nm. This means the fluorescence band will no longer have a simple Gaussian shape, although the wavelengths selected for the FLH measurement are designed to avoid specific absorption features in the atmosphere.

The second process involves physiological changes in the algal assemblage which are another important source of variability in FLH. Light emission by plants *in vivo* is not constant. The natural fluorescence signal per unit chlorophyll under light saturating conditions may vary by almost an order of magnitude (Borstad et al., 1985) and depends principally on species composition, light history, nutrient availability and temperature. At room temperature, most of the observed algal fluorescence arises from photosystem 2 (PS 2). When quantum energy is captured by the algal light harvesting antenna, the energy is mainly used in a first stage to excite chlorophyll units composing the PS 2. From this point there are several possible routes for the decay of the excitation energy. The most important ones are photosynthesis (carbon fixation), thermal dissipation, and fluorescence. The fraction of captured energy used in each one of these processes (quantum yield) is variable. For example, the increase of photoprotective pigments may reduce fluorescence and increase thermal dissipation. Also, nutrient limitation may decrease carbon fixation and raise fluorescence and thermal dissipation. This variation can be caused by changes in light intensity and nutrient stress [Kiefer, 1973 (a); Kiefer, 1973 (b); Abbott et al., 1982], and the response can occur on time scales of a few seconds to several hours. Unfortunately, factors affecting the physiological status of oceanic algal assemblages are difficult, if not impossible, to estimate by remote sensing at present. For this reason we must assess the potential effects that these changes will have in the interpretation of FLH.

The third process affecting interpretation of FLH is the performance of the instrument itself and is the only component that we can control. Thus we will focus our analyses on MODIS and how its performance will affect the behavior of the FLH algorithm.

Sensitivity analyses

The FLH algorithm may be stated as:

$$FLH = L_{14} - L_{baseline} \quad (1)$$

where

$$L_{baseline} = L_{15} + (L_{13} - L_{15}) * [(\lambda_{15} - \lambda_{14}) / (\lambda_{15} - \lambda_{13})]$$

The subscript refers to the MODIS band number (Table 1), L refers to the radiance reading, and λ refers to the band center wavelength (CW). This equation measures the deviation of L_{14} from the baseline calculated using MODIS bands 13 and 15 (Fig. 1). Specifications of the filter spectrum and signal to noise ratio (SNR) for each band are presented in Table 1.

Based on Eq. 1 and assuming that noise is independent between bands, the SNR of the baseline may be calculated as

$$\frac{1}{SNR_{baseline}} = \frac{1}{SNR_{15}} + \left(\frac{1}{SNR_{13}} - \frac{1}{SNR_{15}} \right) * (\lambda_{15} - \lambda_{14}) / (\lambda_{15} - \lambda_{13}) \quad (2)$$

The SNR of the FLH is calculated as:

$$\frac{1}{SNR_{FLH}} = \frac{1}{SNR_{14}} + \frac{1}{SNR_{baseline}} \quad (3)$$

Given the specifications of Table 1, the SNR of FLH is 752.

Fischer and Schlüssel (1990) estimate 8-20 W m⁻² sr⁻¹ μm⁻¹ as a realistic range of upwelling radiance at the top of the atmosphere (TOA) for λ = 685 nm and a solar zenith angle of 50.7°. While the lower radiance of this range corresponds to an atmospheric turbidity factor of 0.5 (visibility = 88 km), the upper value corresponds to a turbidity factor of 10 (visibility = 6 km). A similar value is obtained when the radiance spectrum at the TOA is calculated using a marine atmosphere model with a visibility of 50 km, a solar zenith angle of 60°, and the ocean spectrum without chlorophyll as input datasets for LOWTRAN 4.2 (Kneizys et al., 1988). The upwelling radiance at the TOA for λ = 685 nm

obtained through this method is $8.65 \text{ W m}^{-2} \text{ sr}^{-1} \mu\text{m}^{-1}$. However, given the present characteristics of MODIS band 14, a more accurate estimate of the sensitivity is obtained by using the calculated TOA upwelling radiance at $\lambda = 676.7 \text{ nm}$. In this case, the upwelling radiance at TOA calculated using LOWTRAN becomes $9.05 \text{ W m}^{-2} \text{ sr}^{-1} \mu\text{m}^{-1}$.

The minimum signal of detection (MSD) based on the SNR_{FLH} and the TOA radiance at $\lambda = 676.7 \text{ nm}$ is :

$$MSD = \frac{\text{Radiance}_{\text{TOA}}}{\text{SNR}_{\text{FLH}}} = \frac{9.05 \text{ W m}^{-2} \text{ sr}^{-1} \mu\text{m}^{-1}}{752} = 0.012 \text{ W m}^{-2} \text{ sr}^{-1} \mu\text{m}^{-1}$$

However we should keep in mind that this MSD is calculated for an atmosphere with low turbidity. Under high turbidity, the MSD increases to $0.026 \text{ W m}^{-2} \text{ sr}^{-1} \mu\text{m}^{-1}$ and the sensitivity of the FLH algorithm decreases.

Conversion of FLH into Chlorophyll Concentrations

To convert the MSD into a chlorophyll concentration value, the attenuation effects of the atmosphere path and air-sea interface in the original fluorescence

signal must be taken into account. Furthermore, the potential interference of suspended matter must be considered. Finally, we also must take into account the variability in the fluorescence:chlorophyll ratio.

Assuming a characteristic mid-latitude oceanic atmosphere with a visibility of 23 km, the radiative transfer of the sea surface fluorescence signal measured at $\lambda = 676.7$ nm to the TOA is close to 80%. An increase in the ocean atmospheric aerosol content from a turbidity factor of 0.5 (visibility = 90 km) to a factor of 10 (visibility = 6 km) decreases the absolute atmospheric transfer of the fluorescence signal by less than 30%. Variations in the atmospheric water vapor content also affect the recovery of the TOA fluorescence signal at the TOA by less than 20%. These results are consistent with the results of the analyses performed by Fischer and Schlüssel (1990) using the fluorescence signal at $\lambda = 685$ nm.

Based on the above observations we believe that 30% is a conservative estimate of the loss of the fluorescence signal through the atmosphere. Hence, $0.017 \text{ W m}^{-2} \text{ sr}^{-1} \mu\text{m}^{-1}$ at $\lambda = 676.7$ nm is the minimum fluorescence signal at the ocean sea surface detectable at the TOA by the MODIS FLH algorithm.

Two processes contribute to a decrease of the upwelling radiance when the light crosses the sea-air interface. The principal process is refraction of light at the

sea-air interface. The loss due to this process is approximately 45%. The second process is reflection. The loss in signal is small for angles of 0-40° to the vertical under calm conditions (2-6%) but can increase to 16-27% for the angles in the upper side of this range when the sea-surface becomes rough (Kirk, 1994). By combining both processes, Austin (1980) proposes a correction factor of 0.544 to extrapolate the upwelling radiance at the sea surface to the upwelling radiance just below the surface.

If this correction factor is incorporated in the calculated minimum fluorescence signal measurable at the sea surface, the resulting minimum fluorescence signal in the upper water column required to be detectable from the MODIS platform is $0.032 \text{ W m}^{-2} \text{ sr}^{-1} \mu\text{m}^{-1}$ at $\lambda = 676.7 \text{ nm}$. The conversion of this signal into chlorophyll values will depend on the fraction of energy absorbed by chlorophyll that is released in the form of fluorescence. This fraction is known as the chlorophyll fluorescence quantum yield (Φ_f) so that:

$$FLH = \Phi_f * I_a \quad (5)$$

where I_a is the light flux absorbed by the photosystem. Because most chlorophyll fluorescence originates in PS II, I_a may be approximated by:

$$I_a = I_o * \sigma_{II} * n_{II} \quad (6)$$

where I_o is the mean incident irradiance, σ_{II} is the mean optical absorption of PS II, and n_{II} is the concentration of PS II, having a “typical” value of one unit per 500 chlorophyll *a* molecules (Kolber and Falkowski, 1993). However, under saturated light conditions I_a becomes independent from I_o . If we assume σ_{II} to be constant under light saturated conditions, the light flux absorbed per unit chlorophyll is near constant and the FLH per unit chlorophyll *a* is proportional to Φ_f as follows:

$$\frac{FLH}{Chl.a} = \Phi_f * \frac{I_a}{Chl.a} = cte.*\Phi_f \quad (7)$$

Published values of Φ_f vary between 0.0015 and 0.1 with a mean of 0.0035 (Günter et al. 1986, cited in Fischer and Kronfeld, 1990). However, based on field measurements, a range from 0.002 to 0.02 appears to cover most cases in marine environments (Gordon 1979). Fischer and Kronfeld (1990), assuming $\Phi_f = 0.003$, calculated a conversion factor of 0.05 W m⁻² sr⁻¹ μm⁻¹ per mg chlorophyll at $\lambda = 685$ nm for light saturated photosynthetic conditions. A conversion factor of 0.057 W m⁻² sr⁻¹ μm⁻¹ per mg chlorophyll at $\lambda = 676.7$ nm is found when reconstructing the chlorophyll fluorescence spectrum from the ocean surface

spectra given in Barnes (1994). Using this conversion factor and the calculated detection limit of the fluorescence signal in the upper water column, based on the specified SNR, and the sea surface and atmosphere transmission, the limit of detection of changes in chlorophyll concentration is approximately 0.5 mg m^{-3} (Fig. 2). This limit of detection may decrease to 1.3 mg m^{-3} under turbid atmospheric conditions.

It should be noted that, while atmospheric turbidity may strongly affect the limit of detection of the FLH algorithm by increasing the TOA radiance, the principal potential source of error in the interpretation of changes in the fluorescence signal arises from neglecting the role that algal physiology has in the production of fluorescence. The fluorescence quantum yield (Φ_f) may vary an order of magnitude in marine environments as a result of changes in phytoplankton species composition, nutrient availability, temperature and light. Because under light saturated conditions, the FLH signal per unit chlorophyll is proportional to Φ_f , the detection limit of the FLH algorithm cannot be defined in terms of chlorophyll concentrations unless Φ_f is known. The limit of detection under clear sky conditions may vary from less than 0.3 to greater than $2 \text{ mg chlorophyll m}^{-3}$ when varying the fluorescence to chlorophyll conversion factor from 0.08 to $0.01 \text{ W m}^{-2} \text{ sr}^{-1} \mu\text{m}^{-1}$ per mg chlorophyll (Fig. 2). Furthermore, observed spatial and temporal variations in the FLH signal do not necessarily reflect changes in

chlorophyll concentration unless Φ_f is kept constant. Understanding the variability of the chlorophyll natural fluorescence due to changes in phytoplankton physiology remains a critical step in the interpretation of changes observed in the FLH.

Other parameters that will affect the magnitude of the FLH signal are the size of particles and their effect on scattering, the concentration of suspended matter not containing chlorophyll, and the concentration of yellow substance (Gelbstoff). However, based on the results presented by Fischer and Kronfeld (1990), we have assumed that none of these parameters will modify the FLH by more than 30%. These effects are small compared with the potential variability introduced by changes in the atmosphere turbidity and chlorophyll fluorescence efficiency.

Finally, if noise is independent between pixels the SNR of individual bands increases fourfold when analyzing a 4 by 4 pixel signal. Hence, in areas of the ocean where surface water characteristics are homogeneous over scales larger than 4 by 4 pixels (16 km² at nadir), the limit of detection of chlorophyll concentrations for clear atmospheric conditions, assuming a conversion factor of 0.05 W m⁻² sr⁻¹ μm⁻¹ per mg chlorophyll, decreases to 0.13 mg m⁻³.

Analyses of Band Shifts on Performance of FLH

The above calculation of the sensitivity of the FLH was done based on radiance measured at a single wavelength. E. Knight of NASA/Goddard space Flight Center (1994) produced a detailed analysis of the effect of shifting CW (center wavelength) on the performance of bands 13, 14 and 15 and found that single band performances were affected less than 10% over a range of ± 4 nm when using the normalized filter spectra over the 10 mg chlorophyll *a* m⁻³ Ocean Surface Exitance Spectrum (10-OSES). Even for the 0.01 mg chlorophyll *a* m⁻³ Ocean Surface Exitance Spectrum (0.01-OSES), the effect of shifting center wavelengths is small. Our analyses corroborate these conclusions when using top of the atmosphere (TOA) spectra (Fig. 3). However, the stability of the signal for each one of the bands over an 8 nm range is due to the large contribution to upwelling radiance that is independent of fluorescence. Because the FLH algorithm is designed to remove this contribution (Figs. 1 and 3) variations in the spectral characteristics of the bands may have a stronger effect on the fluorescence signal recovered through the FLH algorithm.

When looking at the TOA spectra for ocean surface waters with 0.01 mg chlorophyll m⁻³, it is clear that FLH will be negative at low or nil chlorophyll concentrations (Fig. 3). The CW of band 15 cannot be shifted towards shorter

wavelengths because of the presence of a water absorption band affecting the 715 to 740 nm range (Fig. 4). Moving this CW towards longer wavelengths will only increase the amount of negativity in the FLH signal without significantly affecting FLH sensitivity. As long as the baseline correction bands are outside the range of the chlorophyll fluorescence signal, the sensitivity of the FLH algorithm is controlled mainly by the position of band 14 with respect to the chlorophyll fluorescence peak.

To decrease the magnitude of the baseline correction and reduce the negativity of the FLH algorithm result at low chlorophyll concentrations, the CW of band 13 could be shifted a few nm toward shorter wavelengths (Fig. 5). This shift would also remove the band 13 range from the chlorophyll fluorescence signal. However, because chlorophyll presents an absorbance band that peaks around 670 nm and interferes with the fluorescence signal, it is useful to have one of the baseline correction bands close to $\lambda = 670$ nm to compensate the FLH signal for chlorophyll absorbance (Fischer and Schlüssel, 1990). At present, the CW of band 13 is at $\lambda = 665.1$ nm and appears to be a good compromise position between compensation for the chlorophyll absorbance effect and maximization of the FLH signal.

As stated above, the sensitivity of the MODIS FLH algorithm is dependent on the position of band 14 with respect to the chlorophyll fluorescence peak. The

absolute value of the FLH result (positive or negative) does not contain information about the sensitivity of the algorithm. To maximize the rate of change of the signal with respect to changes in chlorophyll concentration is the main objective of this analysis. The present CW position of band 14 is located at $\lambda = 676.7$ nm, almost 10 nm away from the chlorophyll fluorescence maximum (Fig. 6). In theory, by shifting the CW of band 14 toward longer wavelengths, while keeping the same baseline correction band positions, the sensitivity of the FLH algorithm can be increased by 40% (Fig. 7). However, oxygen and water absorption bands at wavelengths greater than 686 nm affect the upward radiance (Fischer and Schlüssel, 1990; Fig. 6) introducing variability to the FLH signal. For this reason, the CW position of band 14 could not be increased above $\lambda = 680$ nm (Fig. 6). This shift would still increase the algorithm sensitivity by more than 20% (Fig. 7).

In Fig. 8 we have summarized some of the discussed results by comparing the FLH signal with the actual MODIS band configuration to the signal calculated with the previous specified band configuration (CW = 667, 678, and 748 for bands 13, 14 and 15, respectively). We have performed this analysis for a range of chlorophyll concentrations (0-10 mg) and a range of fluorescence per chlorophyll conversion factors (0.01 to 0.08 $\text{W m}^{-2} \text{sr}^{-1} \mu\text{m}^{-1}$ per mg chlorophyll). In this figure, the slope of the lines at each configuration represents the sensitivity of the FLH algorithm. As expected, the steepest slope correspond to

the situation where fluorescence per unit chlorophyll is maximized and the CW of band 14 is centered at $\lambda = 678$ nm (open squares in Fig. 8). Shifting the CW of bands 13 and 15 upwards 2 nm decreases the absolute FLH value for any given chlorophyll fluorescence signal. However, it has little effect on the sensitivity of the algorithm. From this figure, we can show an extreme example of the effect that the variability in the fluorescence quantum yield has in the interpretation of the FLH signal. Given the present configuration MODIS bands 13, 14 and 15, a FLH signal of $0 \text{ W m}^{-2} \text{ sr}^{-1} \mu\text{m}^{-1}$ may be interpreted as $8.0 \text{ mg chlorophyll m}^{-3}$ or $1.0 \text{ mg chlorophyll m}^{-3}$, depending on the fluorescence conversion factor that is used.

Conclusions

Measurement of FLH from space is clearly challenging. Sensors must have significantly higher SNR than conventional ocean color sensors. Channels must be located precisely, and band position cannot be allowed to shift significantly over the life of the mission. The sophisticated on-board calibration system for MODIS (Guenther et al., in press) will play a key role in the development of the FLH product.

Considering realistic scenarios and given the present specifications of MODIS bands 13, 14, and 15, we are confident that the FLH algorithm will permit the

detection of 1 mg chlorophyll m^{-3} changes in the surface of the ocean. Under optimum viewing conditions, this level can be decreased to 0.5 mg m^{-3} . More oligotrophic regions of the ocean may be studied using FLH if 4 by 4 pixels are averaged together to increase the effective SNR. In this case, the minimum sensitivity improves to 0.13 mg chlorophyll m^{-3} . This sets the minimum chlorophyll concentration under which FLH retrievals can be made. However, we are also interested in the response of the FLH algorithm to changes in chlorophyll concentration. Given the present specifications of MODIS bands 13, 14, and 15, the FLH algorithm sensitivity could be increased by 20% if the center wavelength of band 14 is shifted to $\lambda = 680$ nm from its present position at 676.7 nm.

The FLH algorithm relies on precise band placement to avoid absorption features in the atmosphere as well as to resolve chlorophyll absorbance and fluorescence in the ocean. Subtle shifts in band placement can have a significant impact on the performance of the FLH algorithm. Using chlorophyll concentrations of 10 mg m^{-3} , we calculated the resulting ocean surface exitance spectrum. This spectrum was propagated through the atmosphere using LOWTRAN. Shifts of 4 nm in individual MODIS bands resulted in changes in TOA radiances of less than 2% in individual band performance. However, The FLH absolute signal can be modified by more than 70%. This effect is smaller if bands are shifted the same

amount as a group. Changes in band position in the MODIS instrument are more likely to move bands as a group, rather than move individual bands.

The signal to noise ratio is negatively correlated with atmospheric turbidity and the sensitivity of the FLH signal may vary 3 fold as a result of changes in atmospheric aerosol content. Despite the effects of atmospheric variability, the magnitude of the FLH signal per unit chlorophyll is more dependent on the fluorescence quantum yield of chlorophyll.

The most significant challenge will be the interpretation of FLH data. Assuming that instrument performance and atmospheric variations can be quantified, then variations in the physiological response of the phytoplankton as manifested in their quantum efficiency of fluorescence will be the most important obstacle. However, if chlorophyll concentrations can be estimated independently using radiance ratios, then the variations in FLH over time may be used to derive estimates of quantum efficiency and hence improve models of primary productivity. The next step is to conduct detailed laboratory and field studies to pursue the relationship between FLH and productivity.

References

Austin, R.W. (1980), Gulf of Mexico, ocean-colour surface-truth measurements, *Boundary-layer Meteorol.* 18:269-285.

Abbott, M.R., Richerson, P.J., and Powell, T.M. (1982), In situ response of phytoplankton fluorescence to rapid variations in light, *Limnol. Oceanogr.* 27:218-225.

Abbott, M.R., Brink, K.H., Booth, C.R., Blasco, D., Swenson, M.S., Davis, C.O., and Codispoti, L.A. (1995), Scales of variability of bio-optical processes as observed from near-surface drifters, *J. Geophys. Res.* 100.

Amman, V., and Doerffer, R. (1983), Aerial survey of the temporal distribution of phytoplankton during FLEX'76, In *North Sea Dynamics* (J. Sündermann and W. Lenz, Eds.), Springer-Verlag, Berlin, pp. 517-529.

Barnes, W. (1994) personal communication, NASA, Goddard Space Flight Center, Greenbelt, MD.

Borstad, G.A., Edel, H.R., Gower, J.F.R., and Hollinger, A.B. (1985) Analysis of test and flight data from the Fluorescence Line Imager, *Canadian Spec. Pub. Fish. Aquat. Sci.* 83.

Chamberlin, W.S., and Marra, J. (1992) Estimation of photosynthetic rate from measurements of natural fluorescence: Analysis of the effects of light and temperature, *Deep Sea Res.* 39:1695-1706.

Chamberlin, W.S., Booth, C.R., Kiefer, D.A., Morrow, J.H., and Murphy, R.C. (1990) Evidence for a simple relationship between natural fluorescence, photosynthesis, and chlorophyll in the sea, *Deep Sea Res.* 37:951-973.

Clark, D.K. (1981) Phytoplankton pigment algorithms for the Nimbus-7 CZCS, In *Oceanography from space* (J.F.R. Gower, Ed.), Plenum Press, New York, pp. 227-237

Falkowski, P.G., and Kolber, Z. (1993) Estimation of phytoplankton photosynthesis by active fluorescence, *ICES mar. Sci. Symp.* 197: 92-103.

Fischer, J., and Kronfeld, U. (1990) Sun-stimulated chlorophyll fluorescence 1: Influence of oceanic properties, *Int. J. Remote Sensing* 11: 2125-2147.

Fischer, J., and Schlüssel, P. (1990) Sun-stimulated chlorophyll fluorescence 2: Impact of atmospheric properties, *Int. J. Remote Sensing* 11: 2149-2162.

Fischer, J., Doerffer, R., and Grassl, H. (1986) Factor analysis of multispectral radiances over coastal and open ocean water based on radiative transfer calculations, *Applied Optics* 25: 448-456.

Guenther, B., Barnes, W., Knight, E., Weber, R., Roberto, M., Godden, G., Montgomery, H., and Abel, P. A brief review of the strategy for the at-lunch calibration approach. *Journal for Atmospheric and Oceanic Technology*. (in press).

Gordon, H.R. (1979) Diffuse reflectance in the ocean: The theory of its augmentation by chlorophyll a fluorescence at 685 nm, *Applied Optics* 25: 1161-1166.

Gower, J.F.R. (1980) Observations of in situ fluorescence of chlorophyll *a* in Saanich Inlet, *Boundary Layer Met.*, 18: 235-245.

Gower, J.F.R., and Borstad, G.A. (1981) The information content of different optical spectral ranges for remote chlorophyll fluorescence measurements In *Oceanography from Space* (J.F.R. Gower, Ed.), Plenum Press, New York, pp. 329-338.

Gower, J.F.R., and Borstad, G.A. (1990) Mapping of phytoplankton by solar-stimulated fluorescence using an imaging spectrometer, *Int. J. Remote Sensing* 11:313-320.

Hoge, F.E., Swift, R.N., and Yungel, J.K. (1986) Active-passive airborne ocean color measurements: instrumentation, *Applied Optics* 25: 48-57.

Kiefer, D.A. (1973a) Fluorescence properties of natural phytoplankton populations, *Mar. Biol.* 22:263-269.

Kiefer, D.A. (1973b) Chlorophyll *a* fluorescence in marine centric diatoms: Response of chloroplasts to light and nutrients, *Mar. Biol.*, 23:39-45.

Kiefer, D.A., Chamberlin, W.S., and Booth, C.R. (1989) Natural fluorescence of chlorophyll *a*: Relationship to photosynthesis and chlorophyll concentration in the western South Pacific gyre, *Limnol. Oceanogr.*, 34:868-881.

Kiefer, D.A., and Reynolds, R.A. (1992) Advances in understanding phytoplankton fluorescence and photosynthesis, In *Primary Productivity and Biogeochemical Cycles in the Sea* (P.G. Falkowski and A.D. Woodhead, Eds.), Plenum Press, New York, pp. 155-174.

Kirk, J.T.O. (1994) *Light and Photosynthesis in Aquatic Ecosystems*. 2d Ed, Cambridge University Press, New York, 509 p.

Kishino, M., Sugihara, S., and Okami, N. (1984) Influence of fluorescence of chlorophyll *a* on underwater upward irradiance spectrum, *La Mer* 22:224-232.

Kneizys, F.X., Shettle, E.P., Abreu, L.W., Chetwynd, J.H., Anderson, G.P., Gallery, W.O. , Selby, J.E.A., Clough, S.A. (1988) *Users Guide to LOWTRAN 7*. *Air Force Geophysics Laboratory report # AFGL-TR-88-0177*, 137 p.

Knight, E. (1994) *personal communication*, NASA, Goddard Space Flight Center, Greenbelt, MD.

Kolber, Z., and Falkowski, P.G. (1993) Use of active fluorescence to estimate phytoplankton photosynthesis in situ, *Limnol. Oceanogr.* 38:1646-1665.

Neville, R.A. and Gower, J.F.R. (1977) Passive remote sensing of phytoplankton via chlorophyll fluorescence, *J. Geophys. Res.* 82:3487-3493.

Prezelin, B.B., (1981) Light reactions in photosynthesis, in *Physiological Bases of Phytoplankton Ecology* (T. Platt, Ed.) pp. 1-43, *Can. Bull. Fish. Aquat. Sci.*, 210, pp. 1-43.

Samuelsson, G., and Öquist, G. (1977) A method for studying photosynthetic capacities of unicellular algae based on in vivo chlorophyll fluorescence, *Physiol. Plant* 40:315-319.

Smith, R.C., and Baker, K.S. (1978) Optical classification of natural waters, *Limnol. Oceanogr.* 23:260-267.

Smith, R.C., and Baker, K.S. (1981) Optical properties of the clearest natural waters (200-800 nm), *Appl. Opt.* 20:177-193.

Stegmann, P.M., Lewis, M.R., Davis, C.O., and Cullen, J.J. (1992) Primary production estimates from recordings of solar-stimulated fluorescence in the equatorial Pacific at 150° W, *J. Geophys. Res.* 97:627-638.

Topliss, B.J. (1985) Optical measurements in the Sargasso Sea: Solar-stimulated chlorophyll fluorescence, *Oceanol. Acta*, 8:263-270.

Topliss, B.J., and Platt, T. (1986) Passive fluorescence and photosynthesis in the ocean: Implications for remote sensing, *Deep Sea Res.* 33:849-864.

Table 1. MODIS present specifications for bands 13, 14, and 15.

(from Barnes, 1994).

| MODIS Band # | Center Wavelength | | | Bandwidth | | | Band SNR |
|-----------------|-------------------|-------------------------|---------------------------|-----------|----------------------------|----------------------------|-------------|
| | (nm) | Tolerance up (nm) | Tolerance down (nm) | (nm) | Tolerance upper (nm) | Tolerance lower (nm) | |
| 13 | 665.1 | 1 | 2 | 10.3 | 4.2 | 6.1 | 1368 |
| 14 | 676.7 | 1 | 1 | 11.4 | 5.8 | 5.4 | 1683 |
| 15 | 746.3 | 2 | 2 | 10 | 5.1 | 5.3 | 1290 |

Figure captions:

Fig. 1: Graphical description of MODIS fluorescence line height (FLH) algorithm (dashed and dotted lines represent the normalized transmittance of bands # 13, 14 and 15; Solid lines describe the spectral distribution of upwelling radiance above the surface of the ocean for two selected cases where the chl concentration is 0.01 and 10 mg m⁻³ and the fluorescence per unit chl conversion factor is 0.05 W m⁻² μm⁻¹ sr⁻¹ per mg chl).

Fig. 2: Detection limit of the FLH algorithm on a clear day (visibility = 90 km) as a function of the fluorescence to chlorophyll conversion factor (◆= 0.01, ▲= 0.03, ●= 0.05, ■= 0.08 W m⁻² μm⁻¹ sr⁻¹; values below the dashed line are detectable).

Fig. 3: Baseline correction of the FLH for 0.01 and 10 mg Chl top of the atmosphere spectra.

Fig. 4: Normalized band #15 transmittance superimposed to the top of the atmosphere upwelling radiance spectrum of an ocean surface containing 10 mg chl a m⁻³.

Fig. 5: Normalized band #13 transmittance superimposed to the top of the atmosphere upwelling radiance spectrum of an ocean surface containing

10 mg chl a m⁻³. Dashed lines describe absorbance and fluorescence spectra of chl a in relative units.

Fig. 6: Normalized band #14 transmittance (solid line) superimposed to the top of the atmosphere upwelling radiance spectra of ocean surfaces containing 0.01 and 10 mg chl a m⁻³ (Heavy dashed line describes the difference in upwelling radiance between both TOA spectra).

Fig. 7: Change in the sensitivity of the FLH algorithm as a function of the band #14 center wavelength position.

Fig. 8: Comparison of the FLH response to changes in Chl a concentration relative to the fluorescence : chl a conversion factor for the specified and actual CW band positions (Specified CW positions are 667, 678, and 748 nm for bands #13, 14 and 15, respectively; actual CW positions 665, 676.7, and 746.3).

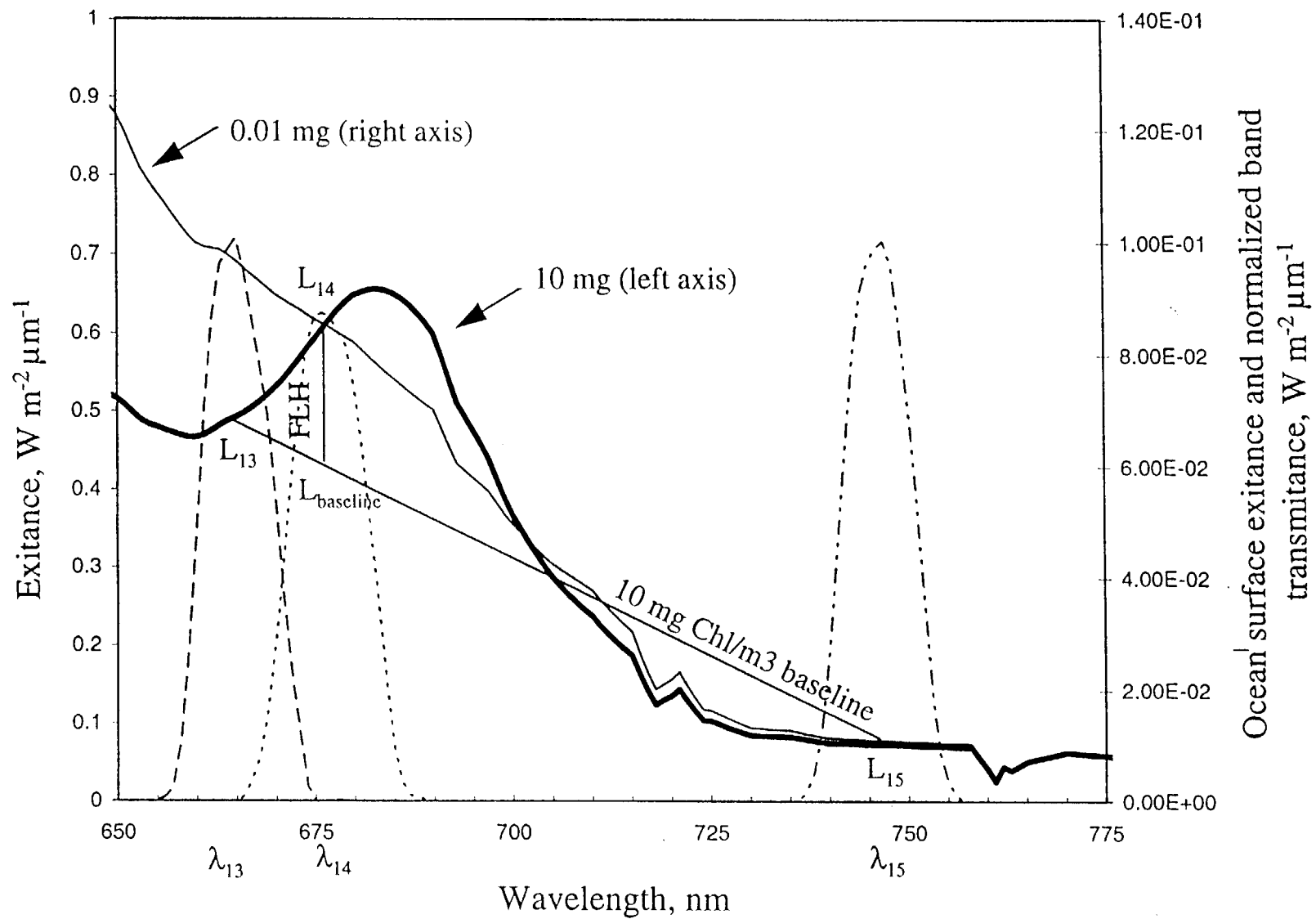


Figure 10: Ocean surface exitance and normalized band transmittance versus wavelength.

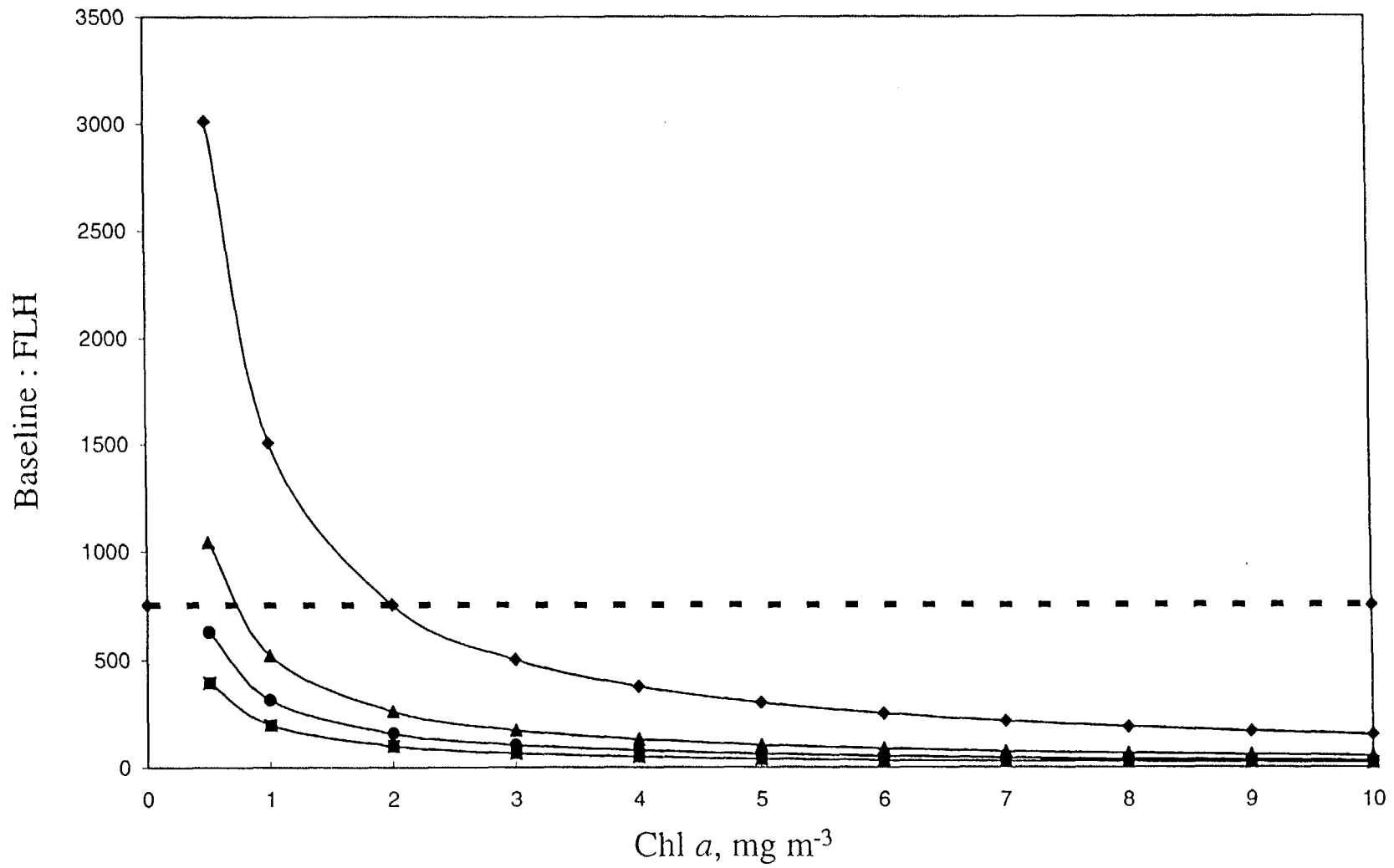


Fig. 2. Lelelie and Abbott

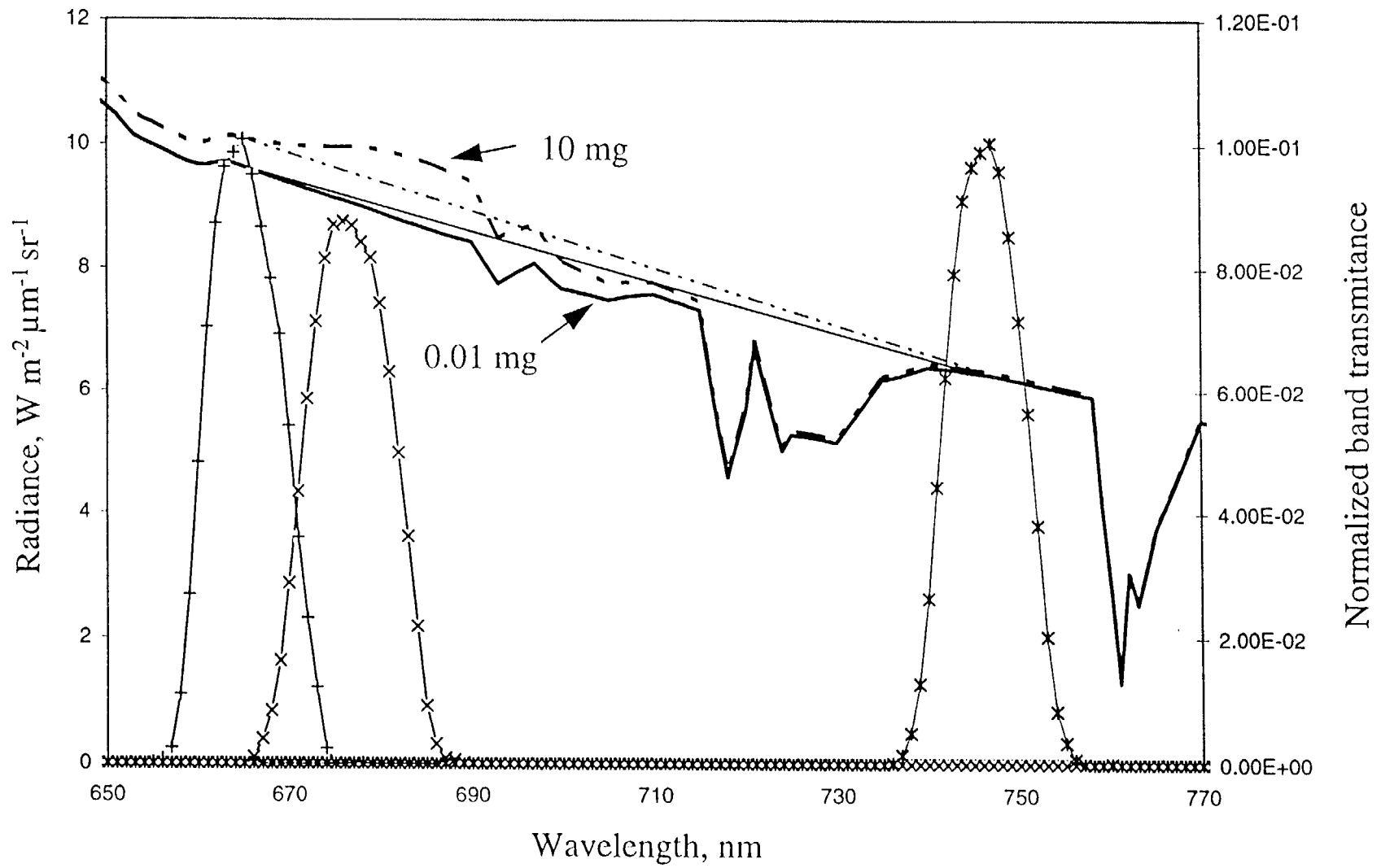


Fig. 2. Radiance and Normalized band transmittance

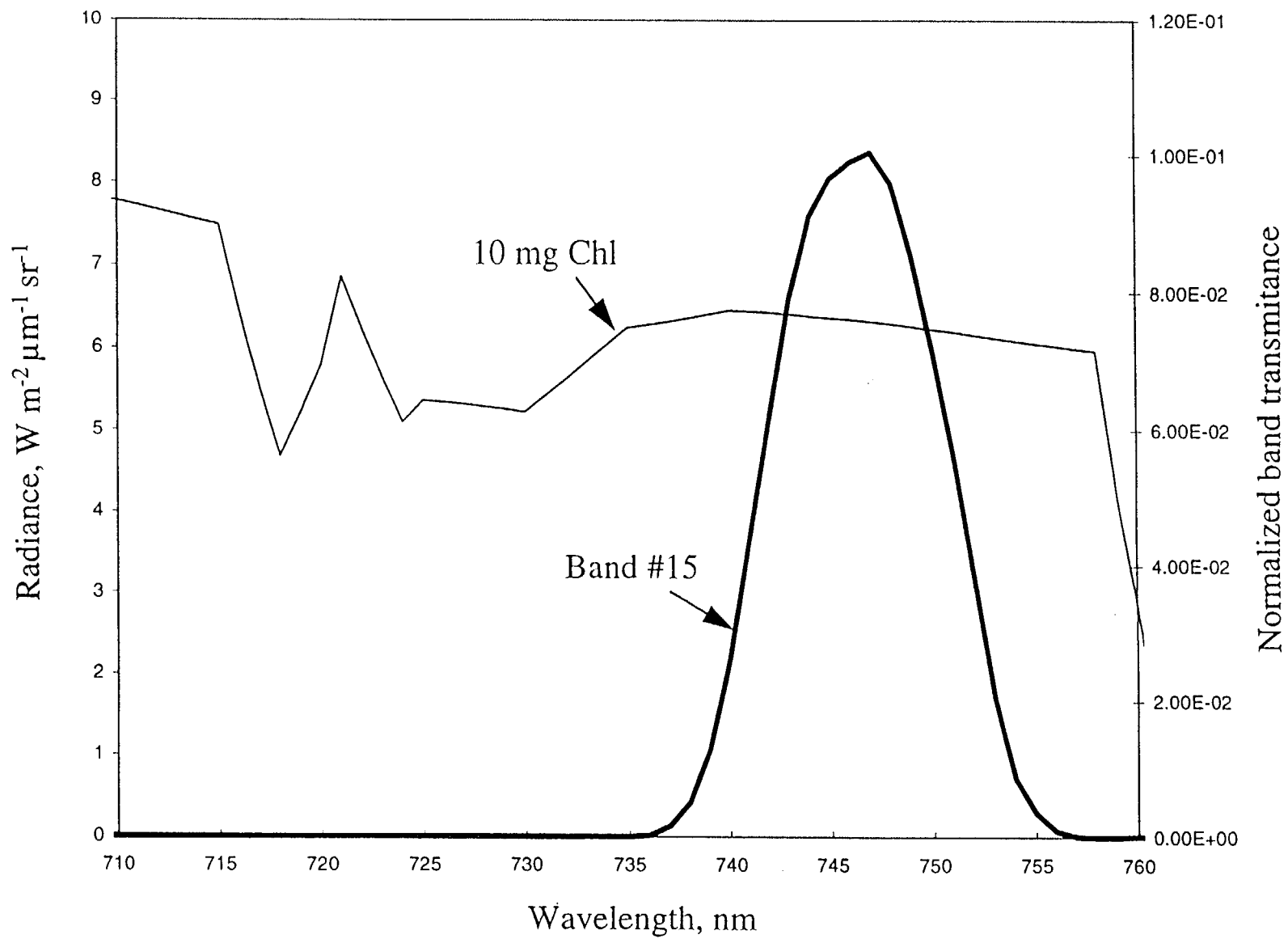


Fig 6, label a and A 1.50

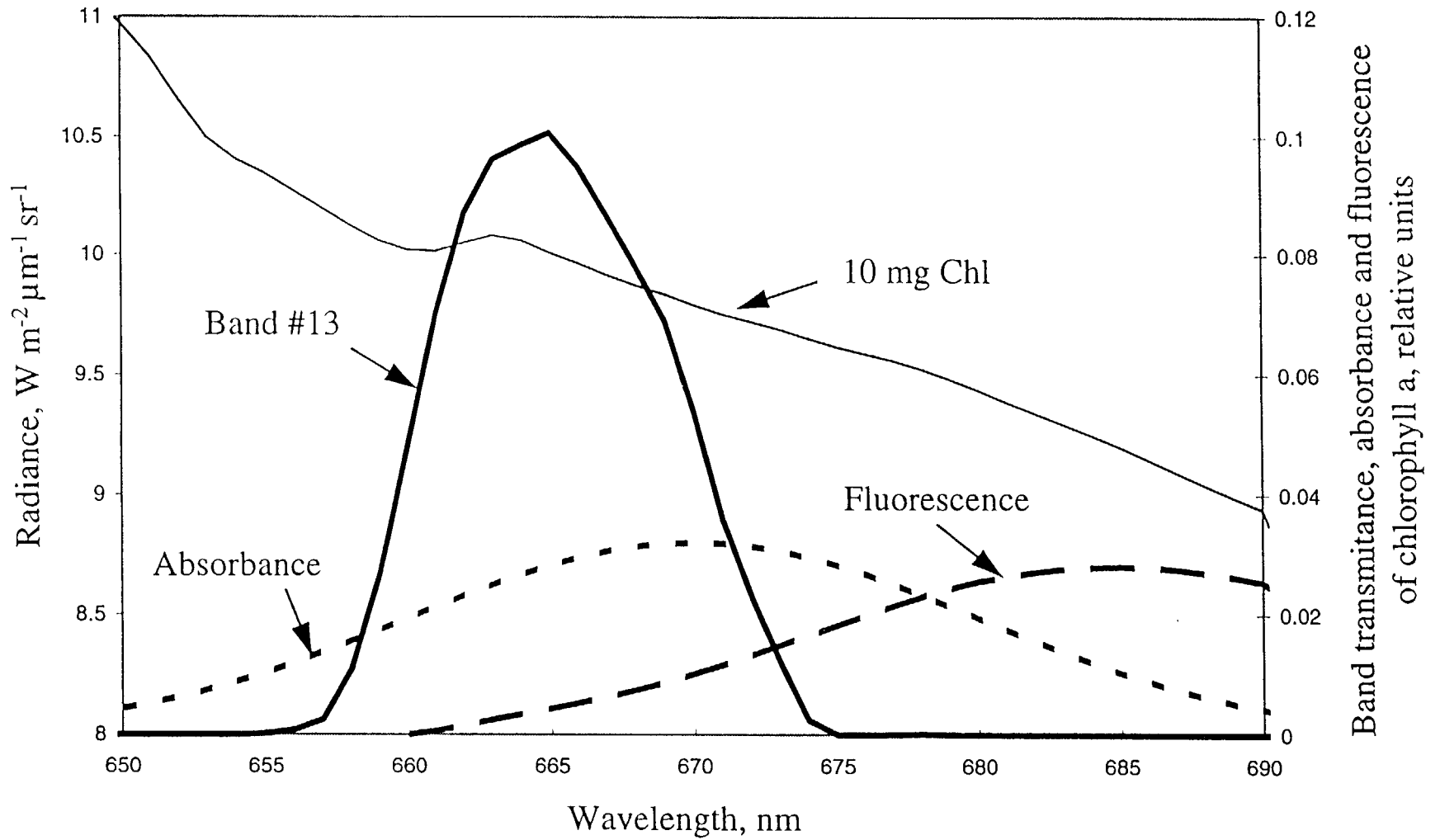


Figure 1. Radiance, absorbance and fluorescence of chlorophyll a.

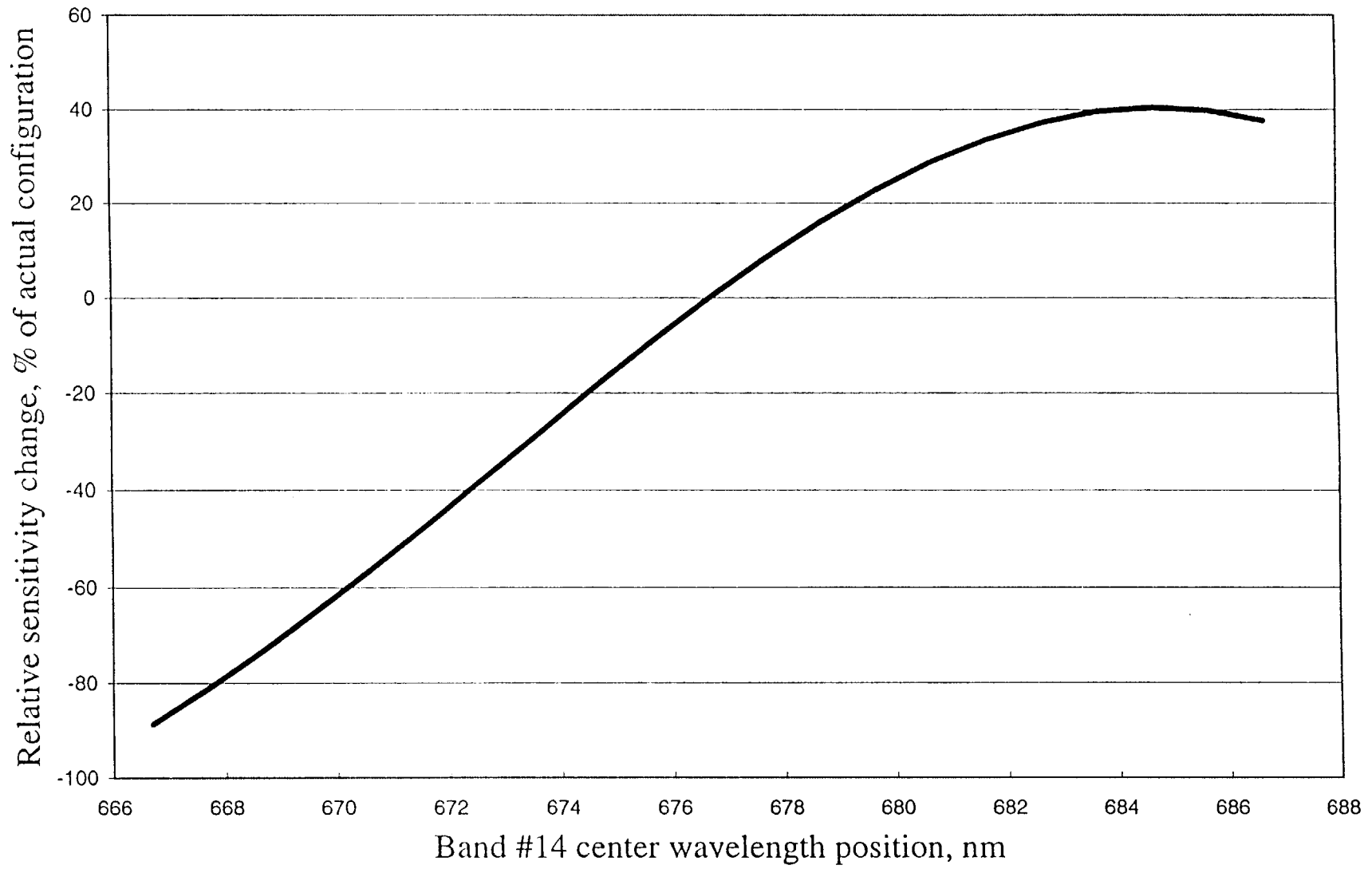


Fig 2. Relative Sensitivity

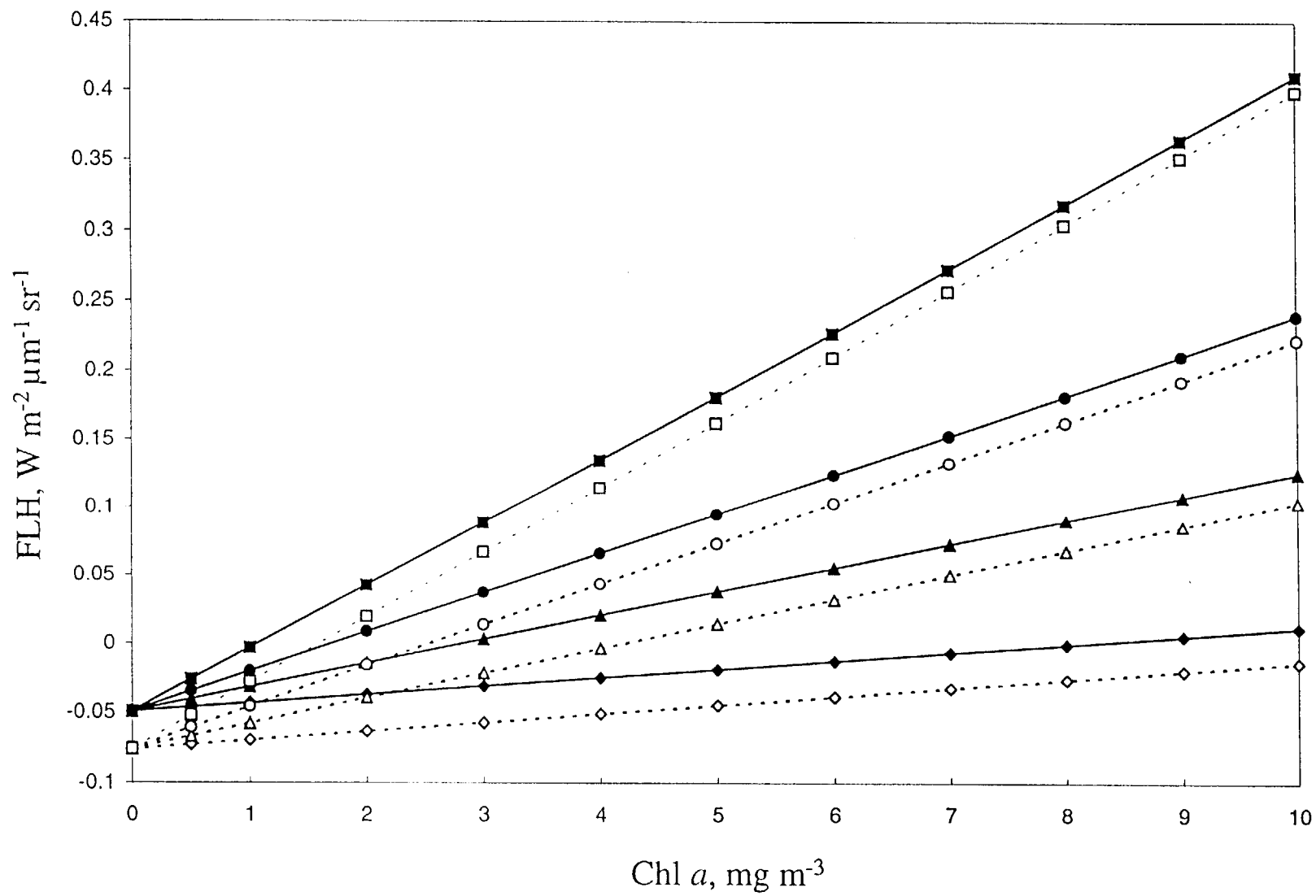


Fig. 2, left, 22 Aug 89